



Research Paper

NUMERICAL INVESTIGATION OF THE HYDRODYNAMIC BEHAVIOR OF THE DEPRESSOR

Jithin P N¹* and Senthil Prakash M N²

*Corresponding Author: Jithin P N, ✉ jithinpnarayanan@gmail.com

Many oceanographic applications require an underwater body to be towed at a specified water depth. But because of the tow cable force the underwater towed body may tend to come to the towing vessel level. Depressor is a device that gives a depressive force on the underwater towed body and helps it to be towed at a particular depth. There are many forms of the depressors designed with different configurations for the purpose. Hydrodynamic depressors are those which provide the depressive force derived from the negative lift created by the depressor wings. This paper presents the CFD analysis of a hydrodynamic depressor carried out using the software FLUENT. The incompressible Reynolds averaged Navier-Stokes equation with Standard *k-v* turbulence model is solved to estimate hydrodynamic performance of the depressor. The characteristics such as lift and drag forces, lift and drag coefficients, velocity and pressure distribution around the wings and body of the depressor are evaluated at a negative angle (angle that gives a lift component of force in the downward direction) of attack. The CFD results are compared with available experimental results and are found to be matching in close tolerance.

Keywords: Angle of Attack (AOA), Computational Fluid Dynamics (CFD), Depressor, Depressive force, Standard *k-v* turbulence model

INTRODUCTION

The oceanographic applications such as sea bed mapping and ocean environment investigation and naval application including acoustic detection of a submerged target and mine detection, require an underwater body or vehicle to be moved in the ocean at a pre-

determined depth. This is usually facilitated by towed cable array system. The towing systems possible are single part towing system and two part towing system.

Single part towing system is a conventional underwater towed system which consists of a towing cable connecting the towed body with

¹ Department of Ship Technology, Cochin University of Science and Technology, Cochin 682022, Kerala, India.

² Division of Mechanical Engineering, CUCEK, Cochin University of Science and Technology, Cochin 682022, Kerala, India.

the towing vessel. One of the disadvantages of single part towing system is that the towed body becomes shallow as the towing vessel speed increases. This can only be adjusted by increasing the tow cable length. But increasing the tow cable length increases the cable tension, drag force and hence requires a massive array handling system. Many schemes have been put forward to maintain an underwater towed vehicle to move stable while operating under different towing speeds. One of these is to use a two part underwater towed system.

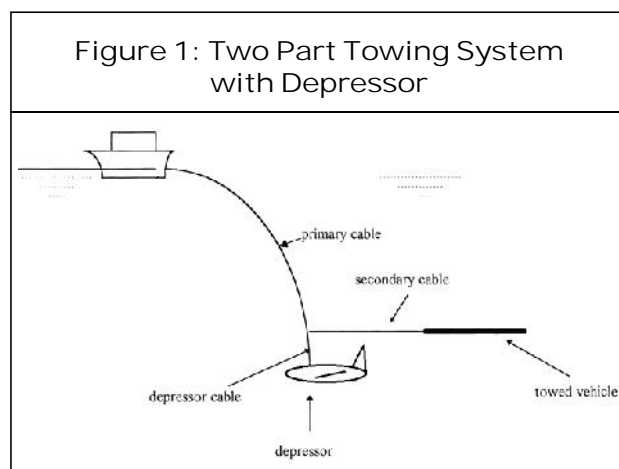
A two part towing system shown in Figure 1 consist of a depressor connected to the main tow cable, followed by another connecting cable and a tow-fish, which are both close to neutral buoyancy. The hydrodynamic design of the wings and body of the depressor will provide sufficient depressive force (negative lift) to the towed body and helps in preventing the towed body from rising to tow vessel level at higher towing speeds. It helps in maintaining the towed body at the required depth. Also it decouples the towed body from the induced ship motions and ensures its stability. It is possible to attain more depth with the same cable length by

using a depressor. It is also effective for a wide range of towing speeds.

The principles and design of the underwater towed bodies and depressors have been developed and investigated by many researchers by different methods. Dessureault (1976), Hopkin *et al.* (1993) and Jiaming and Chwang (2000) mentioned in the reference shows the efforts by some researchers in this area. Becker (1950) in his report describes a program directed towards the development of a high speed, light weight depressor for towing a sonar array from surface ships. The report covers the design, fabrication and model basin test of a half scale model and also the design, fabrication, model basin test and at sea test of a full scale model. Results of the test program have verified the performance and demonstrated the ease of handling a light weight depressor.

CFD has become a useful tool for analysis of most of the marine hydrodynamic problems Anantha Subramanian and Senthil Prakash (2010) and Arun Kumar and Senthil Prakash (2013). Senthil Prakash and Subramanian (2010), Senthil Prakash and Deepti R Nath (2012), and Senthil Prakash and Binod Chandra (2013) shows some of the applications of CFD in marine hydrodynamics. In the current paper the numerical analysis of the prototype depressor mentioned in Becker (1950) is described. The numerical investigation is conducted using the Computational Fluid Dynamics software FLUENT.

The hydrodynamic coefficients, pressure and velocity distributions of the depressor at various speeds are investigated using CFD and compared with experimental results.



DEPRESSOR MODEL SPECIFICATION

Proper hydrodynamic design is necessary in order to achieve the effective performance of a depressor. A non-hydrodynamic shape can cause excessive drag, noise and instability even at low speeds. The external shape of a depressor is important for minimizing the energy required to move the vehicle through the water at the required speed for the desired range.

The geometric specifications of the depressor model used for the hydrodynamic analysis is the one which is mentioned in the report of R.F. Becker that covers the work performed by the EDO Corporation in design, fabrication and test of a high speed towed sonar array depressor program Becker(1950). National Advisory Committee for Aeronautics (NACA) 0012 to 0018 are symmetric profiles generally

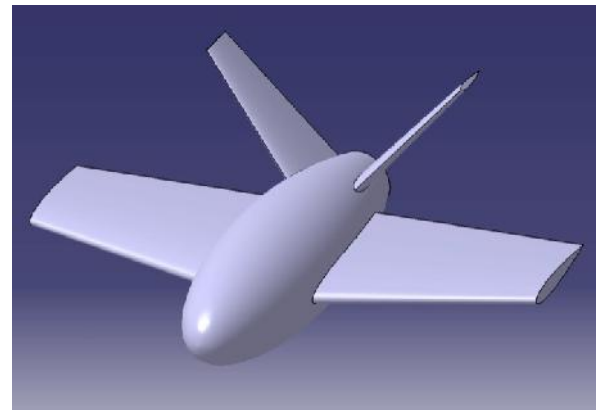
used for wing sections of depressors. The depressor which is modeled has a NACA 0015 section fixed main wings; with a 4.50 negative incidence on a truncated DTMB EPH shaped body. The tail wings have V configuration and NACA 0015 cross section with a 00 incidence. As described in Wilburn (1962) the dimensionless offsets of the fore body and after body of DTMBEPH shaped body of the depressor is prepared. Table 1 shows the general geometric specification of the depressor.

Model for Simulation

The 3D geometric model of the depressor is made using CATIA V5. Figure 2 shows the 3D view of the depressor developed in CATIA V5. This model for analysis need to be enclosed in a domain of suitable size.

Table 1: Geometric Specification of the Depressor	
Depressor Body	
Body Shape	DTMB EPH
Reference length	889mm
Max. body diameter	254 mm
Length from nose to tail trailing edge	775mm
Main Wing	
Wing cross section	NACA 0015
Wing span	1143mm
Incidence	4.50 leading edge down
Tail Wing	
Wing cross section	NACA 0015
Span	305mm
V configuration	Trailing edges 450 from vertical
Incidence	00

Figure 2: 3D Model of the Depressor



NUMERICAL ANALYSIS OF DEPRESSOR

Computational Fluid Dynamic (CFD) analysis is carried out to investigate the hydrodynamic coefficients, pressure and velocity distributions on the surface of the depressor and to examine the performance of the depressor at varying speeds and Angles Of Attack (AOA). The CFD

simulations for the depressor are conducted by using FLUENT.

Governing Equations

The general conservative form of the Navier-Stokes equation is given below.

Continuity equation,

$$\frac{\partial \rho}{\partial t} + \frac{\partial}{\partial x_i}(\rho u_i) = 0 \quad \dots(1)$$

where, ρ = density, u_i is the velocity component in the i^{th} direction ($i = 1, 2, 3$). The flow around the depressor is considered three dimensional steady state and incompressible. The density is constant in case of incompressible flows and so the continuity equation gets modified as,

$$\frac{\partial}{\partial x_i}(\rho u_i) = 0 \quad \dots(2)$$

Momentum or Navier- Stokes equation,

$$\frac{\partial}{\partial t}(\rho u_i) + \frac{\partial}{\partial x_j}(\rho u_j u_i) = -\frac{\partial p}{\partial x_i} + \frac{\partial \tau_{ij}}{\partial x_j} + \rho g_i \quad \dots(3)$$

where, τ_{ij} is the Reynolds stress tensor given by,

$$\tau_{ij} = \left[-\left(\frac{\partial u_i}{\partial x_j} + \frac{\partial u_j}{\partial x_i} \right) \right] - \frac{2}{3} \rho \frac{\partial u_l}{\partial x_l} u_{ij} \quad \dots(4)$$

p = static pressure, g_i = gravitational acceleration in the i^{th} direction, δ_{ij} is the Kroneker delta and is equal to unity when $i = j$; and zero when $i \neq j$. The Reynolds-Averaged form of the above momentum equation including the turbulent shear stresses is given by,

$$\frac{\partial}{\partial t}(\rho U_i) + \frac{\partial}{\partial x_j}(\rho U_j U_i)$$

$$= \frac{\partial}{\partial t}(\rho U_i) + \frac{\partial}{\partial x_j}(\rho U_j U_i) - \frac{\partial p}{\partial x_i} + \frac{\partial}{\partial x_j} \left(-\rho \overline{u'_i u'_j} \right) \quad \dots(5)$$

where,

u'_i = instantaneous velocity component,

$\left(-\rho \overline{u'_i u'_j} \right) = R_{ij}$ is called the Reynolds stress.

For the closure of the RANS equation a turbulence model is used (Standard k - ϵ turbulence model). The standard k - ϵ turbulence model is the most widely employed two- equation eddy- viscosity model. It is based on the solution of equations for the turbulent kinetic energy and the turbulent dissipation rate. Equations (6) and (7) are used to determine the lift and drag forces (F_L and F_D) respectively.

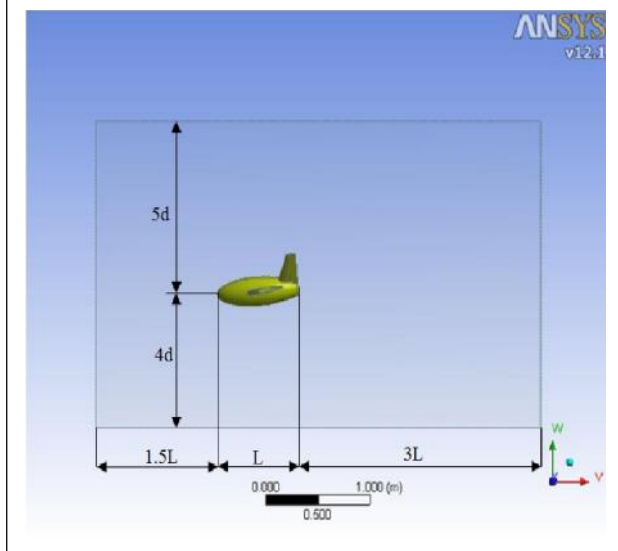
$$F_L = \frac{1}{2} \times \rho \times v^2 \times A \times C_L \quad \dots(6)$$

$$F_D = \frac{1}{2} \times \rho \times v^2 \times A \times C_D \quad \dots(7)$$

where, C_L is the lift force, C_D is the drag force, ρ is the density of the fluid medium, v is the velocity of the fluid and A is the reference area chosen for calculating lift and drag force. In this case the wing area is considered to be the reference area and it is 0.372 m².

Domain specifications and meshing
The sea (fluid domain) in which the depressor is moving is modeled as a rectangular prism with dimensions as described below. The fluid domain extends to 1.5 times the length of the depressor body upstream and 3 times the depressor length downstream in the axial direction. Depth of the depressor below free

Figure 3: Domain Specifications



stream is taken as the dimension of the domain height above the depressor. The depth below the depressor is fixed to be 4 times the maximum diameter of the depressor. The width of the domain is fixed by taking the wing span to both sides from the wing tips (i.e., 1143 mm). The details of the domain length and height are shown in the Figure 3.

During the preprocessing the meshing of the depressor with unstructured mesh is carried out. The discretized domain is shown in Figure 4.

Unstructured meshing allows meshing of complex geometry with in lesser time. The flow around the depressor too close to the body is of interest. So an inflation layer option (providing high quality mesh) is used to mesh this region , where the boundary layer around the body is present. The unstructured tetrahedral mesh and the fine layers of mesh created around the depressor surface are shown in the Figure 5. More than 300000 cells with a skewness value of 0.38 have been generated during meshing.

Figure 4: Unstructured Mesh in Fluid Domain

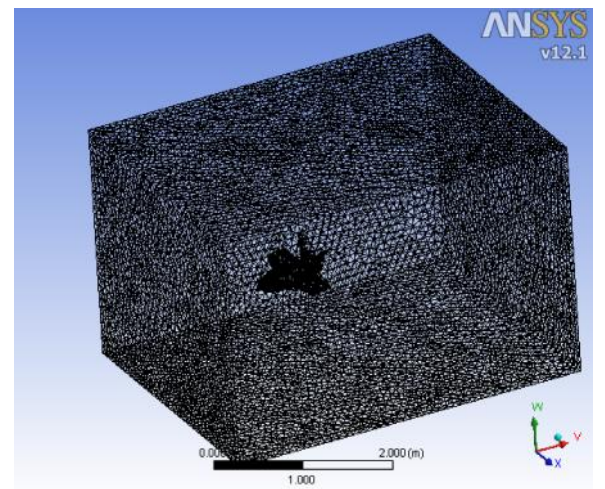
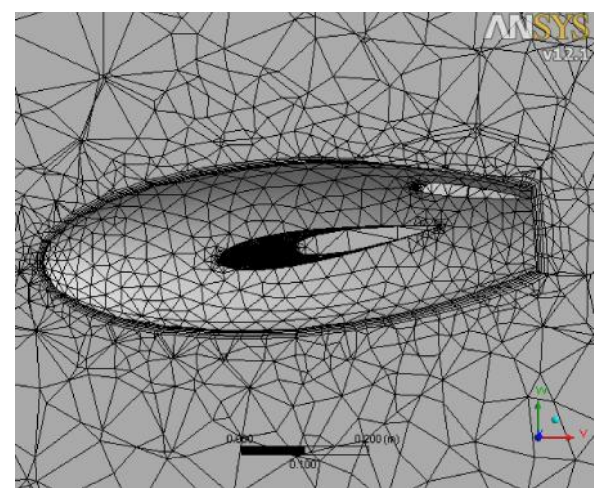


Figure 5: Tetrahedral Meshing with Inflation Layer



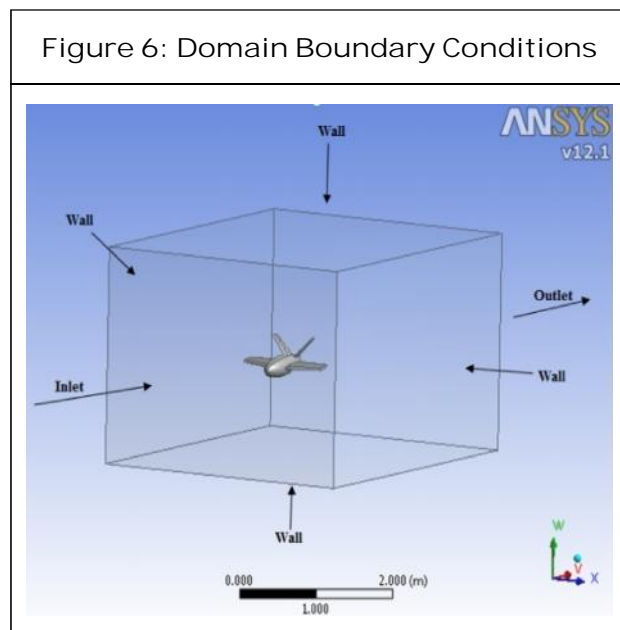
Solver Settings

Solver parameters for the simulation of depressor were set considering the general recommendations and the specific ones obtained from simulation trials done on the model. Standard *k-v* turbulence model with SIMPLE scheme for the pressure-velocity coupling. The solver parameters and physical constants used in the simulation are shown in Table 2.

Description	Details
Type of solver	Pressure based-SIMPLE scheme
Turbulence model	Standard k-v
Inlet flow velocity (Tow velocity)	2.57 m/s-23.15 m/s
Density of water	1000 kg/m ³
Viscosity of water	0.001003 kg/m-s

Boundary Conditions

The boundary conditions considered are, for inlet- velocity inlet that ranges from 2.57 m/s-23.15 m/s, for outlet-pressure outlet and for the domain walls-wall with no slip condition is applied. Figure 6 shows the boundary conditions applied.



RESULTS AND DISCUSSION

During the CFD analysis of the depressor at negative wing angle of attack (leading edge down) of 8.5°, it was found that the depressive force and lift coefficient obtained at 35 knots speed are 7096.12 pounds and 0.524 respectively. The negative lift (depressive force) is mainly generated by the body and

main wings of the depressor. The depressive force and the drag provided by the depressor having a negative wing AOA of 8.5° at varying speeds, obtained from CFD analysis is shown in the Figures 7 and 8. The CFD results are compared with experimental results of model basin test conducted by EDO Corporation Becker (1950) as a standardization step. The CFD results were found very close to the experimental results.

Figure 7: Lift vs Speed with 8.5° Negative AOA of Main Wings-CFD

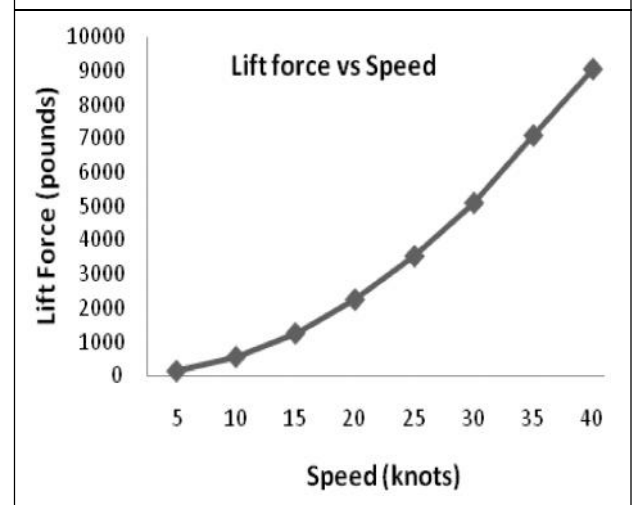


Figure 8: Drag vs Speeds 8.5° Negative AOA of Main Wings-CFD

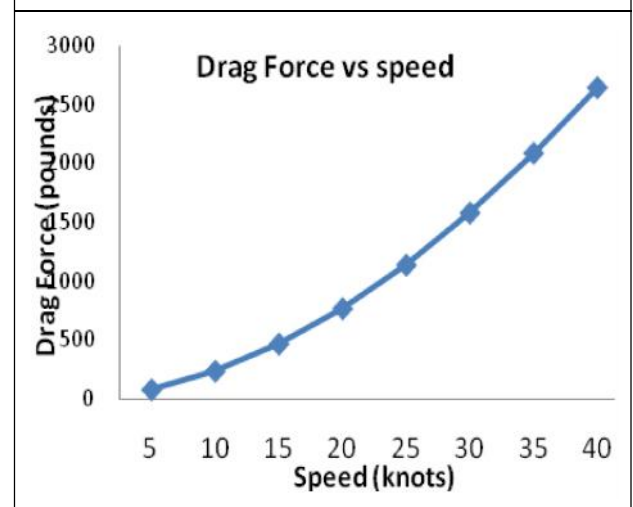


Table 3: CFD Results Compared with Available Experimental Results

Parameter	CFD Result	Experimental Result Becker (1950)
CL (Lift Coefficient)	-0.5239	-0.5
Depressive force (Pounds) speed	7096.12	7000

Figures 9 to 13 shows the pressure distribution on the surface of the depressor at

Figure 9: Front View of the Pressure Distribution at 45 Knots and -8.5° AOA

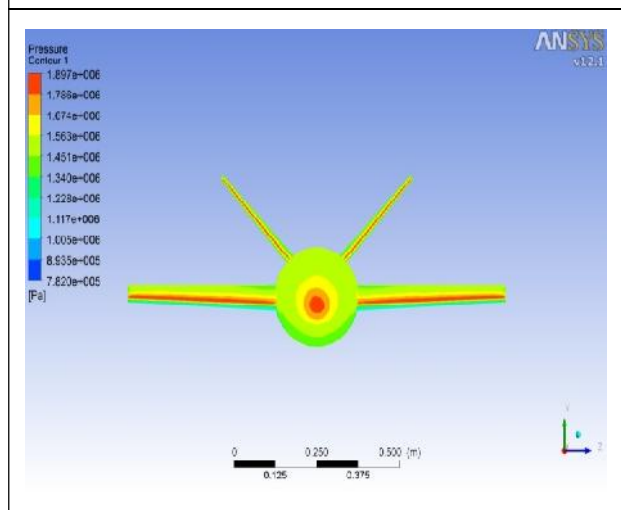


Figure 10: Top View of the Pressure Distribution at 45 Knots and -8.5° AOA

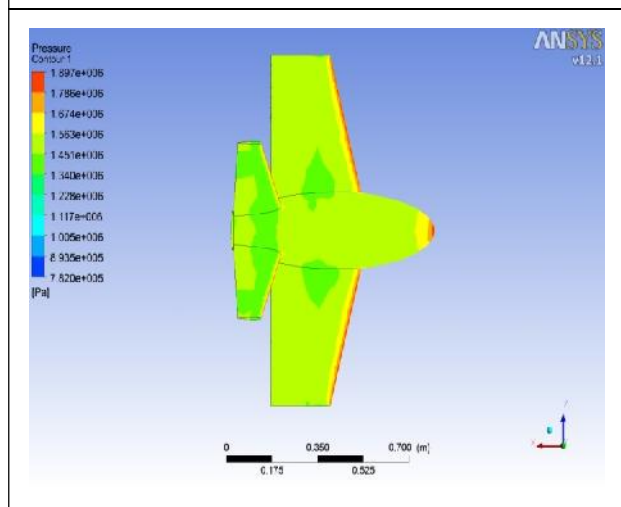


Figure 11: Bottom View of the Pressure Distribution at 45 Knots and -8.5° AOA

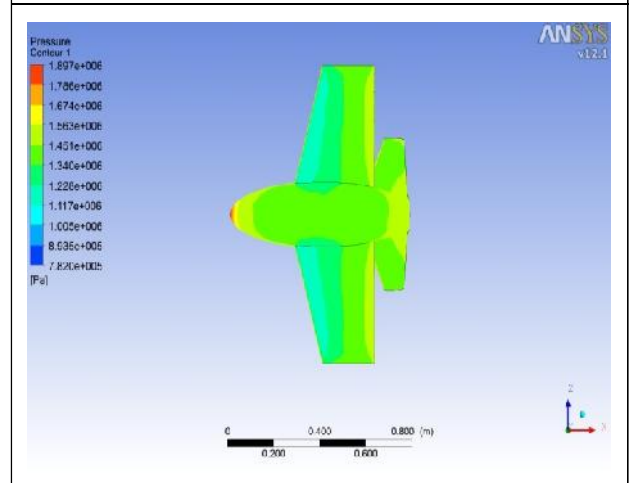


Figure 12: Pressure Contour of the Depressor Body at 45 Knots and -8.5° AOA

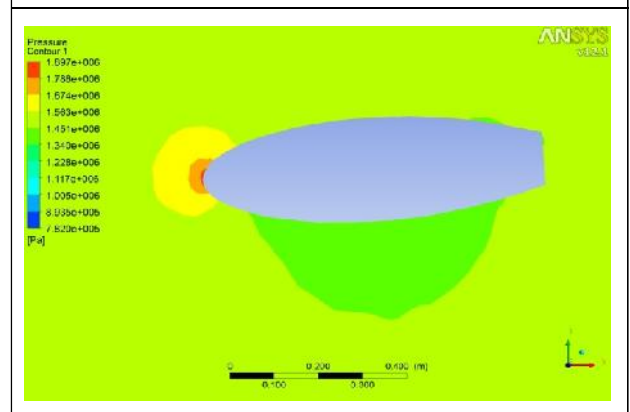
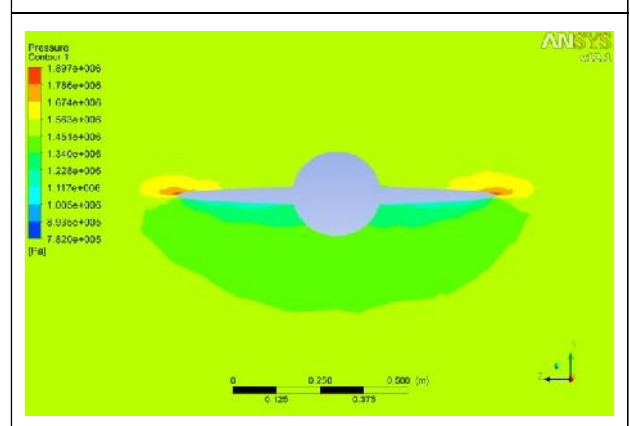


Figure 13: Pressure Contour of the Depressor



45 knots. It can be observed from the figures that because of the negative AOA provided for the wings and the body a low pressure region is created on the bottom surface of the body and main wings of the depressor. This provides sufficient depressive force for the depressor at high speeds.

It can be observed from the Figures 9-13 that at 45 knots (23.15 m/s) with the wing having a negative angle of attack of 8.5°, a maximum pressure of about 1897 KN/m² is observed at the nose of the depressor body and at the leading edges of the wings

(represented by dark red colour). A low pressure region is created at the bottom surface of the wings and the body (represented by blue colour), which causes the depressor to have a negative lift.

Figures 14 and 15 shows the velocity variation on the body and main wings of the depressor at 45 knots (23.15 m/s) with the wings having a negative AOA of 8.5°. The maximum velocity observed is 30.72 m/s (represented by the dark red region in the velocity contour) at the bottom of wings. The velocity is zero near to the depressor surface, at the nose of the depressor body and at the wing leading edge.

Figure 14: Velocity Contour of the Depressor Body at 45 Knots and -8.5° AOA

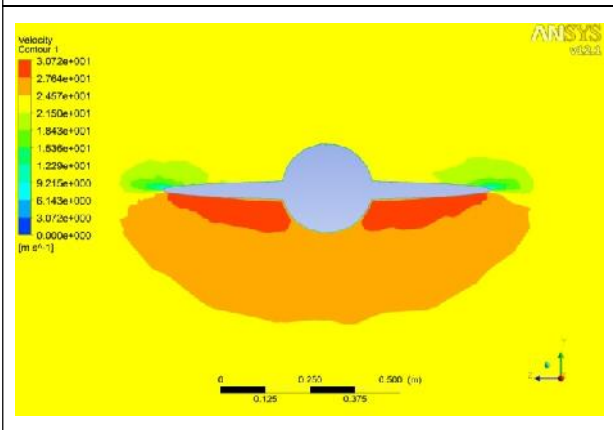
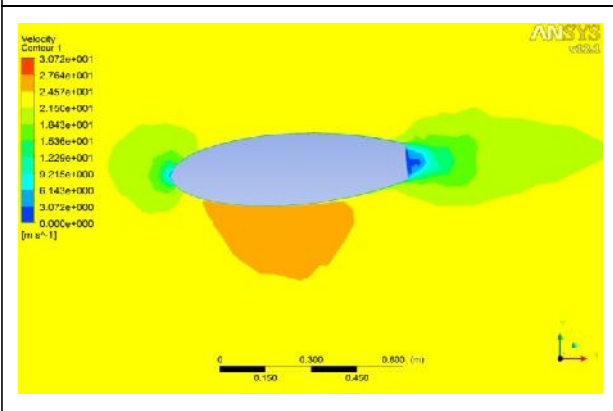


Figure 14: Velocity Contour of the Depressor main wings at 45 Knots and -8.5° AOA



CONCLUSION

A two part towing system with hydrodynamic depressors provide depressive force (negative lift) to the towed body and prevents the towed body from rising to the free surface at higher towing speeds. It thus maintains the towed body at a constant depth. Numerical analysis has been performed on a selected prototype depressor using the CFD package FLUENT aimed at studying the hydrodynamic behavior at various tow speeds.

The simulation results carried out at 35 knots and at a wing angle of attack of 8.5 degree (leading edge down) could be compared with the published experimental results of the depressor program conducted by EDO Corporation Becker (1950). The depressive force obtained from CFD analysis was 7096 pounds against the experimental result of 7000 pounds, which are in close tolerance. Thus the effort to numerically simulate the depressor for its hydrodynamic performance has been proved successful. 🌀

REFERENCES

1. Anantha Subramanian V and Senthil Prakash M N (2010), "Optimization of Propeller by Coupled VLM and RANS Solver Method", 7th International Conference on High-Performance Marine Vehicles Melbourne, October 13-15, Florida, USA.
2. Arun Kumar K K and Senthil Prakash M N (2013), "Numerical Investigation on the Hydrodynamics of Flow Over Submarine Petroleum Pipes", *Indo-American Journal of Mechanical Engineering*, December, In Press.
3. Becker R F (1950), "High Speed Sonar Array Depressor Program Final Report", Prepared for Office of Naval Research, Virginia.
4. Chapman DA (1984), "A Study of the Ship Induced Roll Motion of a Heavy Towed Fish", *Ocean Engineering*, Vol. 11, No. 6, pp. 627-654.
5. David Hopkin, Jon M Preston and Sonia Latchman (1993), "Effectiveness of a Two-Part Tow for Decoupling Ship Motions", *Defence Research Establishment Pacific, IEE*, pp. 1359-1364.
6. Dessureault (1976), "Bat Fish a Depth Controllable Towed Body for Collecting Oceanographic Data".
7. Jiaming Wu and Allen T Chwang (2000), "Experimental Investigation on a Two-Part Underwater Towed System", *Ocean Engineering*, Vol. 28, March, pp. 735-750.
8. Senthil Prakash M N and Deepti R Nath A (2012), "Computational Method for Determination of Open Water Performance of a Marine Propeller", *International Journal of Computer Applications*, Vol. 58, No. 12, pp. 1-5.
9. Senthil Prakash M N and Binod Chandra (2013), "Numerical Estimation of Shallow Water Resistance of a River-Sea Ship Using CFD", *International Journal of Computer Applications*, Vol. 71, No. 5, pp. 33-40.
10. Senthil Prakash M N and Subramanian V A (2009), "Body Force Based Simulation of Propeller Hull Interaction", 3rd International Conference In Ocean Engineering, ICOE 2009, February 1-5, Chennai.
11. Senthil Prakash M N and Subramanian V A (2010), "Simulation of Propeller-Hull Interaction Using Rans Solver", *The International Journal of Ocean and Climate Systems*, Vol. 1, pp. 189-208.
12. Wilburn L Moore (1962), "Bodies of Revolution with High Cavitation-Inception Speeds—for Application to the Design of Hydrofoil-Boat Nacelles".